Dynamic features of successive upwelling events in the Baltic Sea – a numerical case study

OCEANOLOGIA, 52 (1), 2010.
pp. 77–99.

KEYWORDS
Upwelling
Baltic Sea
Hel Peninsula
Numerical modelling

Kai Myrberg[1,⋆]
Oleg Andrejev[1]
Andreas Lehmann[2]

[1] Finnish Environment Institute/Marine Research Centre,
Mechelininkatu 34a, FIN–00251 Helsinki, Finland;

e-mail: Kai.Myrberg@ymparisto.fi

⋆corresponding author

[2] Leibniz Institute of Marine Sciences,
Düsternbrooker Weg 20, D–24105 Kiel, Germany

Received 21 October 2008, revised 18 January 2010, accepted 22 January 2010.

Abstract

Coastal upwelling often reveals itself during the thermal stratification season as an abrupt sea surface temperature (SST) drop. Its intensity depends not only on the magnitude of an upwelling-favourable wind impulse but also on the temperature stratification of the water column during the initial stage of the event. When a 'chain' of upwelling events is taking place, one event may play a part in forming the initial stratification for the next one; consequently, SST may drop significantly even with a reduced wind impulse.

Two upwelling events were simulated on the Polish coast in August 1996 using a three-dimensional, baroclinic prognostic model. The model results proved to be in good agreement with in situ observations and satellite data. Comparison of the simulated upwelling events show that the first one required a wind impulse of 28 000 kg m^{-1} s^{-1} to reach its mature, full form, whereas an impulse of only 7500 kg m^{-1} s^{-1} was sufficient to bring about a significant drop in SST at the end of the second event. In practical applications like operational modelling, the initial stratification conditions prior to an upwelling event should be described with care in order to be able to simulate the coming event with very good accuracy.

1. Introduction

Upwelling is an important process in the World Ocean. It is also a well-known and important factor in Baltic Sea physics. The main mechanism producing upwelling is wind forcing. Since the Baltic Sea is a semi-enclosed, relatively small basin, winds from virtually any direction blow parallel to some section of the coast, giving rise to coastal upwelling there. During the thermal stratification period, upwelling can lead to a sudden sea surface temperature drop of more than 10°C, abruptly changing the thermal balance and stability conditions at the sea surface. Upwelling can additionally play a key role in replenishing the euphotic zone with the nutritional components necessary for biological productivity when the surface layer is depleted of nutrients. In general two classes of upwelling can be distinguished: open-sea and coastal upwelling. The first class is of considerably larger scale and includes such vertical motions as those caused by the wind (Ekman pumping), and effects of the main oceanic thermocline and equatorial ocean currents. Coastal upwelling is regionally more limited than open ocean upwelling but its stronger vertical motion is associated with a greater climatic and biological impact. Vertical motions in coastal upwelling are of the order of 10^{-5} m s^{-1}, in open ocean upwelling they are about 10^{-6} m s^{-1}, which corresponds to 1 m day^{-1} and 0.1 m day^{-1} respectively (Dietrich 1972 ed.). Coastal upwelling could be defined as the vertical movement of water masses compensating for the offshore Ekman drift, but oceanographers often include in this term the consequences of this vertical movement in stratified waters. For example, Csanady (1977) uses the term 'full' upwelling when the vertical movement is intensive and sufficiently long-lasting to move the thermocline up to the surface. The same idea is incorporated in multi-layer models of upwelling (Cushman-Roisin 1994). In this paper we are going to retain this broader interpretation of the term 'upwelling'. The reverse of upwelling is called downwelling; this is associated with surface convergence and divergence in a lower layer where the water's descent terminates. Downwelling does not manifest itself so clearly at the sea surface and does not have such biological relevance as upwelling (for details, see Lehmann & Myrberg 2008).

How, then, can we find out where upwelling takes place? There are many ways to investigate it. In summer, a rapid and abrupt drop in SST is a key parameter, indicating that upwelling may be taking place. The distribution of vertical velocity is also a good parameter for studying upwelling, especially when numerical models are available (Myrberg & Andrejev 2003). In the case of upwelling, the vertical velocity is always directed upwards in the areas of interest. However, there are considerable difficulties with estimating vertical velocities from measurements. The distribution of water

density is not such a good indicator because in the Baltic Sea the effect of temperature on density is not as pronounced as that of salinity. Moreover, the main upwelling events in the Baltic usually take place in coastal areas where the vertical distribution of salinity is quite homogeneous and thus, no great changes in sea water density are expected to take place in connection with upwelling (Leppäranta & Myrberg 2009).

In this paper we focus on the investigations of the dynamics of two upwelling events occurring off the coast of the Hel Peninsula, Poland, in August 1996. Our study is based on high-resolution three-dimensional baroclinic hydrodynamic model simulations. The motivation of the study is the following: the mesoscale dynamics of upwelling in the Baltic Sea is still not fully understood, hence further investigations are an ongoing activity. The most recent steps in modelling studies are to be found in the papers by Zhurbas et al. (2008) and Laanemets et al. (2009). For the Gulf of Finland these authors used the Princeton Ocean Model with a very high-resolution (ca 0.5 nm $\times$ 0.5 nm). They found interesting mesoscale features of upwelling with filaments and squirts. We continue here to analyse mesoscale features in the current and temperature fields related to coastal upwelling. It will be shown later on that the estimate of the upwelling extension given by a two-layer reduced-gravity model (the qualitative analysis of this model is presented in Cushman-Roisin 1994) is, not surprisingly, close to our results. Simple two-layer models take into account the main mechanisms causing upwelling – the Ekman offshore drift and geostrophic adjustment. Such a simplified two-layer approach also helps us to understand the specific features of vorticity distribution in the upwelling area.

A measure of the winds capable of causing upwelling is the wind impulse, which can be estimated by integrating the wind stress over the duration of the event (Cushman-Roisin 1994, Haapala 1994). How upwelling manifests itself depends on the stratification and the strength of the wind impulse; the main aim of this paper is therefore to describe, by using numerical modelling and measurements, the role of initial temperature stratification in the development of upwelling. This important subject has so far not been studied extensively in the Baltic Sea. The numerical simulations for summer 1996 in the southern Baltic show how wind impulses of rather different magnitudes can cause a significant drop in the sea surface temperature, and how this in turn depends on the temperature stratification during the early development of the upwelling.

The structure of the paper is as follows. Section 2 describes the numerical model with its experimental set-up. The case study for summer 1996 is introduced with the data sets used for the model run and its

verifications. After that, the results of wind impulse calculations for different upwelling-favourable wind events are presented. The main model results are analysed in Section 3 – this starts with a verification of the model using satellite images and in situ data. Since no current measurements are available for the model verification, we show that the dynamics of the simulated upwelling is in agreement with the simple two-layer approach. After that we describe how successive upwelling events are affected by previous ones. The study concludes with a summary and a review of some of the practical consequences of the investigation.

2. Material and methods

2.1. The model

The numerical model, developed by Andrejev & Sokolov (1989, 1990), is of the time-dependent, free-surface, baroclinic, three-dimensional type, using traditional simplifications: the hydrostatic approximation, an incompressibility condition, a Laplacian closure hypothesis for sub-grid scale turbulent mixing, and the β-plane approximation. Since the reader will find a detailed description of the model in, for example, Myrberg & Andrejev (2003), Andrejev et al. (2002, 2004a,b), and Myrberg & Andrejev (2006), we describe the model here only in brief.

The model used here was recently validated against an extensive data set in the Gulf of Finland in 1996 with encouraging results. Additionally, the results of six hydrodynamic models, including the model used here, for the Gulf of Finland have been inter-compared with a thorough statistical analysis of the results (Myrberg et al. 2010).

Main parameters and assumptions

The horizontal kinematic eddy diffusivity coefficient was calculated using the formula of Smagorinsky (1963). The vertical eddy diffusivity coefficient was taken to depend on the local velocity shear and stratification (Kochergin 1987). Wind stress was described by the well-known quadratic law following Niiler & Kraus (1977), and the drag coefficient at the sea-surface was formulated according to Bunker (1976). A quadratic law was used for the bottom friction, where the drag coefficient was prescribed as 0.0026 (Proudman 1953). Heat fluxes at the sea-surface were calculated in the same way as suggested in the COHERENS-model (see http://www.mumm.ac.be/~patrick/mast/).

Set-up of the numerical model experiments

The numerical simulation covers the period from 1 July 1996 until 31 August 1996. The applied 1x1 nautical mile bathymetry is based on Seifert & Kayser (1995). However, a slightly changed coastline (taken from navigational maps) was constructed for the Hel Peninsula area to take into account specific topographic features there, which are not described accurately enough in the standard topography.

The open boundary of the model domain was placed in the Kattegat along latitude 57°35′N. In order to properly prescribe the sea level in the Kattegat, observations were needed from both ends of the open boundary, namely, one observation point on the Swedish side and one on the Danish side. An active free radiation condition (Orlanski 1976, Mutzke 1998) was used for the Kattegat sea level and the respective sea level measurements at Göteborg (Sweden) and Fredrikshamn (Denmark) at 1 h intervals. The horizontal resolution for the entire Baltic Sea model – 1 nautical mile in both horizontal directions – is suitable to describe mesoscale dynamics; this is scaled by the internal Rossby radius, which varies between 3 and 10 km in this area (see e.g. Fennel et al. 1991). The model comprised 44 levels in the vertical with a layer thickness increasing monotonically towards the bottom (2.5 m for the upper layer, 5 m intervals down to 152.5 m, and below that depth 10 m intervals). We used the Swedish Meteorological and Hydrological Institute's (SMHI) gridded meteorological data (wind speed and direction, air temperature, cloudiness, relative humidity and precipitation) for the simulation period with a spatial resolution of 1 degree for the entire Baltic Sea area and with a temporal resolution of 3 hours. Since the wind velocities in the data set represent geostrophic values only, these were reduced to represent 10 m values. A standard method for this correction is to multiply the wind speed by a factor of 0.6 and deflect the direction 15° anticlockwise (Bumke & Hasse 1989). We used the Data Assimilation System and Baltic Environmental Database (Sokolov et al. 1997) for constructing the initial temperature and salinity fields. The mean monthly river discharges for 1970–90 (Bergström & Carlsson 1994, Sokolov et al. 1997) were used. Altogether 29 rivers were taken into account in the entire Baltic model. Runoff from small rivers was added to the discharges of the main rivers.

2.2. Verification data

SST maps were kindly made available by the Federal Maritime and Hydrographic Agency (BSH, Hamburg Germany) and were processed operationally from infrared high resolution data of the U.S. NOAA weather satellite series. The accuracy of the SSTs is about ±0.2°C.

Additionally CTD measurements carried out during a hydrographic survey by the Polish r/v 'Baltica' (Baltic Environmental Database http://nest.su.se/bed/) in August 1996 were used to validate the simulated results of upwelling.

2.3. Wind conditions and wind impulse for upwelling events in August 1996 on the Polish coast

On the Polish coast upwelling is favoured when a high pressure system is located over north-western Russia, which gives rise to light or moderate easterly to south-easterly winds over the southern Baltic (Bychkova & Viktorov 1987, Malicki & Wielbińska 1992, Lehmann & Myrberg 2008). The

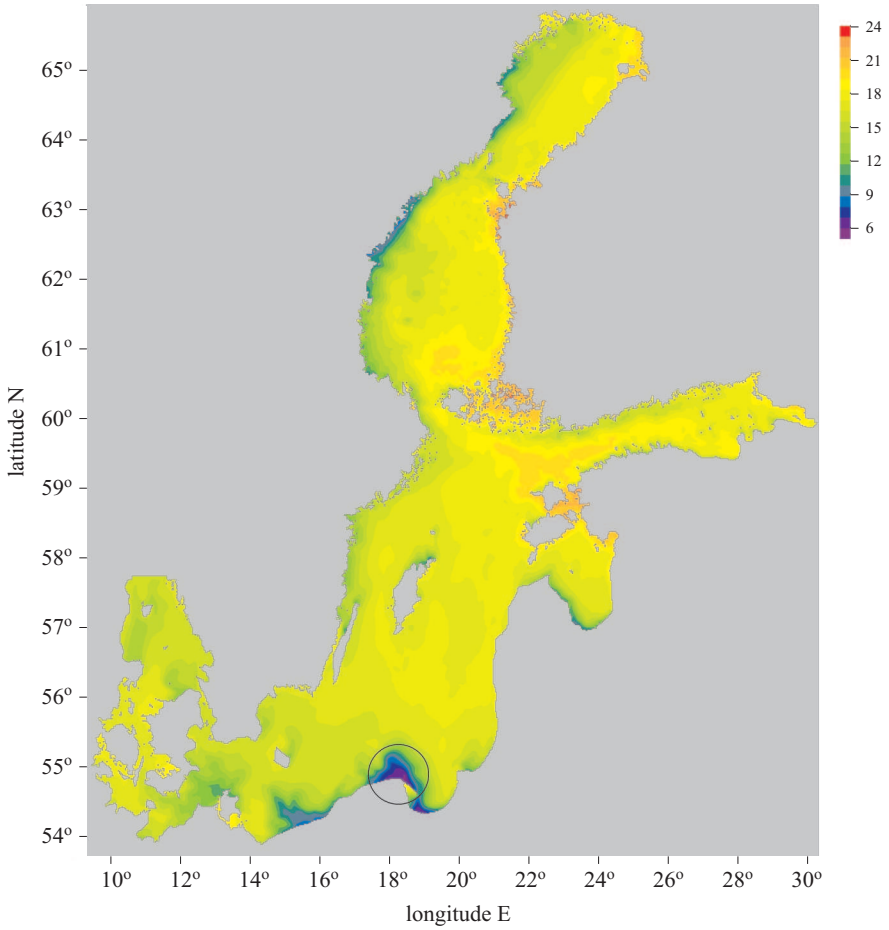

Figure 1. The calculated sea surface temperature on 13 August 1996. The location of the upwelling area under investigation is marked with a circle

area of interest is located off the Hel Peninsula (Figure 1). On the basis of a seven-year numerical model simulation Kowalewski & Ostrowski (2005) recently found that wind directions favourable to upwelling on the Polish coast range from 45° to 180°, i.e. winds blowing from north-east to south (Figure 2).

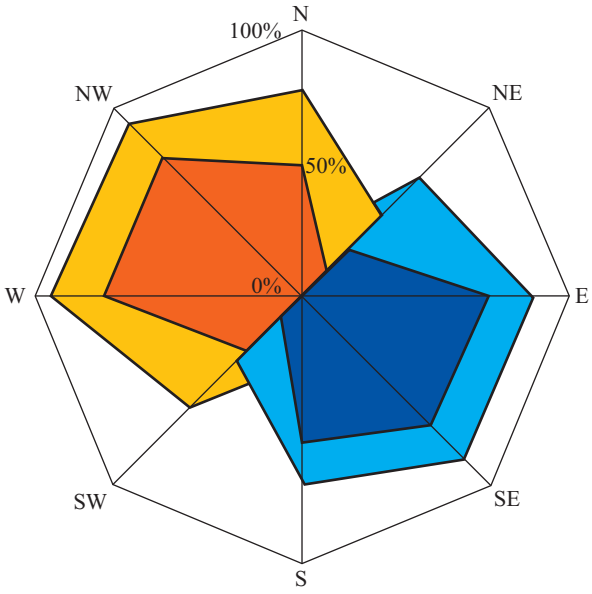

Figure 2. Probability of upwelling (blue, dark-blue) and downwelling (yellow, orange) events, depending on the wind direction near the Hel Peninsula (redrawn from Kowalewski & Ostrowski 2005)

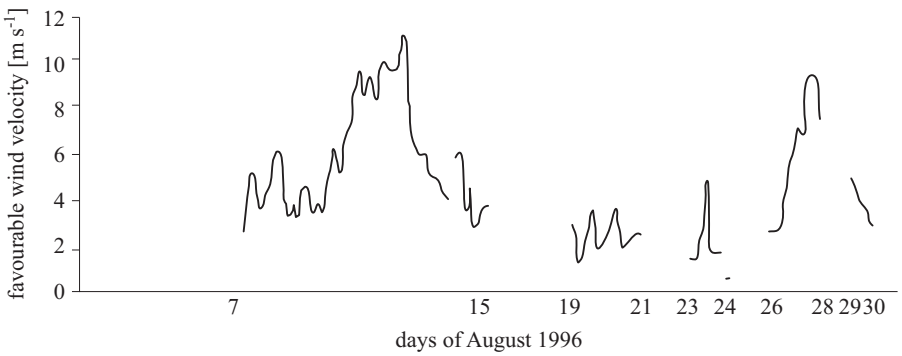

Figure 3. Wind velocities [m s^{-1}] favourable (from between 45° and 180°) to upwelling at the SMHI gridded data point nearest to the Hel Peninsula in August 1996

Figure 3 shows the time periods of winds favourable (blowing from between 45° and 180°) to upwelling at the SMHI gridded data point nearest to the Hel Peninsula in August 1996. It turned out that there were many

different periods with different lengths from one day to about one week, when upwelling-favourable winds were blowing. Wind speeds were typically around 5 m s^{-1}, reaching a maximum of about 12 m s^{-1}.

In the Gulf of Gdańsk, upwelling has most often been found to take place off the Hel Peninsula (see e.g. Matciak et al. 2001). The potential maximum upwelling area on the Polish coast amounts to 10 000 km^2, which is ca 30% of the Polish economic zone (Krężel et al. 2005).

Following Cushman-Roisin (1994) and Haapala (1994), the wind impulse as the integration of the wind-stress over time is:

$$I = \int_0^t \tau_a \, dt' = \int_0^t C_a \, \rho_a \, U_a^2 \, dt', \tag{1}$$

where ρ_a is the air density, C_a the drag coefficient, U_a the wind speed at 10 m height and t the wind duration. Table 1 gives the dates when an upwelling-favourable wind started to blow and the duration of such a wind event in hours. The corresponding wind impulses I were calculated according to equation (1) using the SMHI gridded meteorological data (geostrophic wind corrected to represent a 10 m wind according to Bumke & Hasse 1989) at the grid point nearest the Hel Peninsula.

Table 1. Periods of winds favourable to upwelling, their duration (h) and wind impulse (in kg m^{-1} s^{-1}) off the Hel Peninsula in August 1996 calculated using equation (1) with SMHI gridded data

Start of event	Duration [h]	Wind impulse [kg m^{-1} s^{-1}]
7 August	228	36 000
19 August	66	1800
23 August	28	700
26 August	42	7500
29 August	12	120

It turned out that the wind impulse for the first case, beginning on 7 August, was very large (36 000 kg m $^{-1}$ s^{-1}) due to the quite high wind speed (mostly between 5 and 11 m s^{-1}) and the long duration of the wind event (Figure 3). After that, there were two short periods of upwelling-favourable winds, starting on 19 August (wind impulse 1800 kg m^{-1} s^{-1}) and on 23 August (wind impulse 700 kg m^{-1} s^{-1}), which did not produce any noticeable SST drop (Figure 4). Between 26 and 28 August upwelling-favourable winds were again blowing with speeds of up to 10 m s^{-1} and an impulse equal to 7500 kg m^{-1} s^{-1}, which caused a significant upwelling.

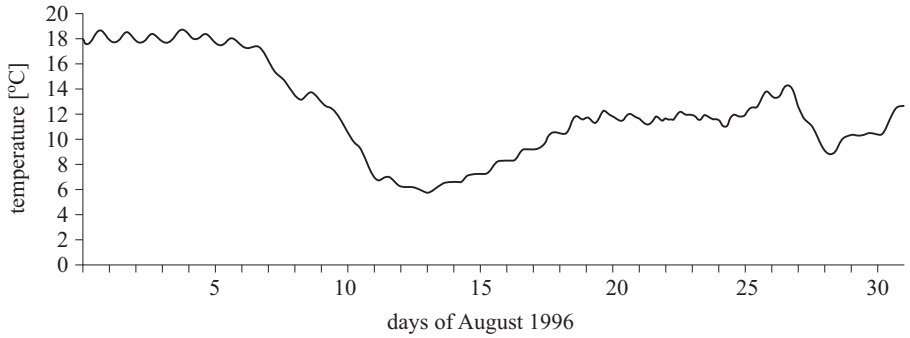

Figure 4. The time series of the calculated sea surface temperature near the Hel Peninsula, August 1996. The temperature is given in °C, the time in days

3. Results

3.1. Verification of model results

The calculated sea-surface temperature on 13 August (Figure 1) and the SST of the satellite image – a composite of satellite overpasses from

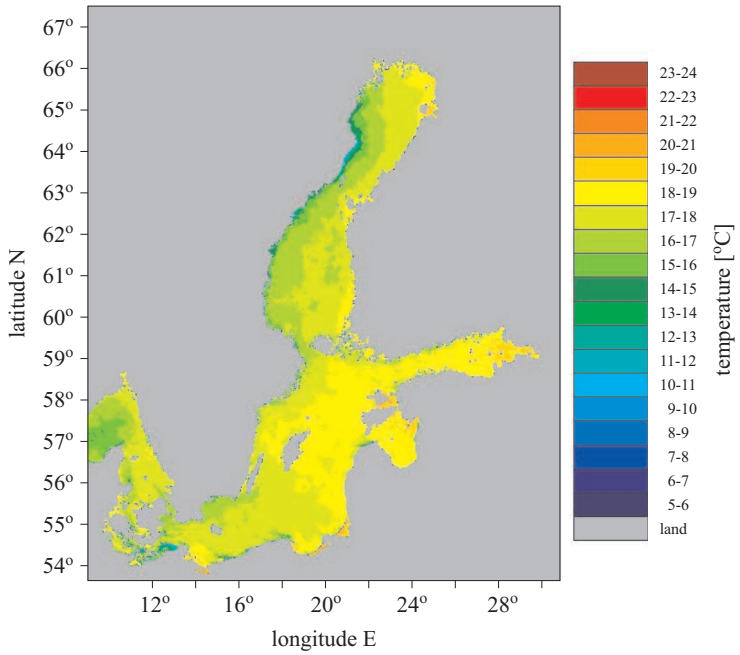

Figure 5. Satellite image of the sea surface temperature – a composite of satellite overpasses from 7–13 August 1996

7–13 August 1996 (Figure 5) – resemble one another closely. Both images show a wide strip of cold water along the western coast of the Baltic – the similarity is especially significant for the Gulf of Bothnia – and they also demonstrate traces of upwelling off both the northern and southern coasts of the Gulf of Finland. Upwelling also becomes visible off the coasts of the islands of Gotland, Bornholm and Rügen.

The evident resemblance in upwelling shape and the good correspondence in sea surface temperature distribution is demonstrated by comparison of Figures 6 and 7: the former shows the calculated sea surface temperature on 13 August for the Hel Peninsula area, the latter shows the satellite image for the same area and day. The shape and extension of the upwelling area off the Hel Peninsula is well described by the model. However, even when the model's resolution is high, the frontal areas are somewhat too diffusive. The model-produced upwelling in the southern corner of the Gulf of Gdańsk and west of the Curonian Spit is much less strongly developed in the satellite data. This is because the model lacks a detailed description of the Vistula Lagoon. Another possibility might be the inaccuracies in the wind forcing data used (SMHI gridded data).

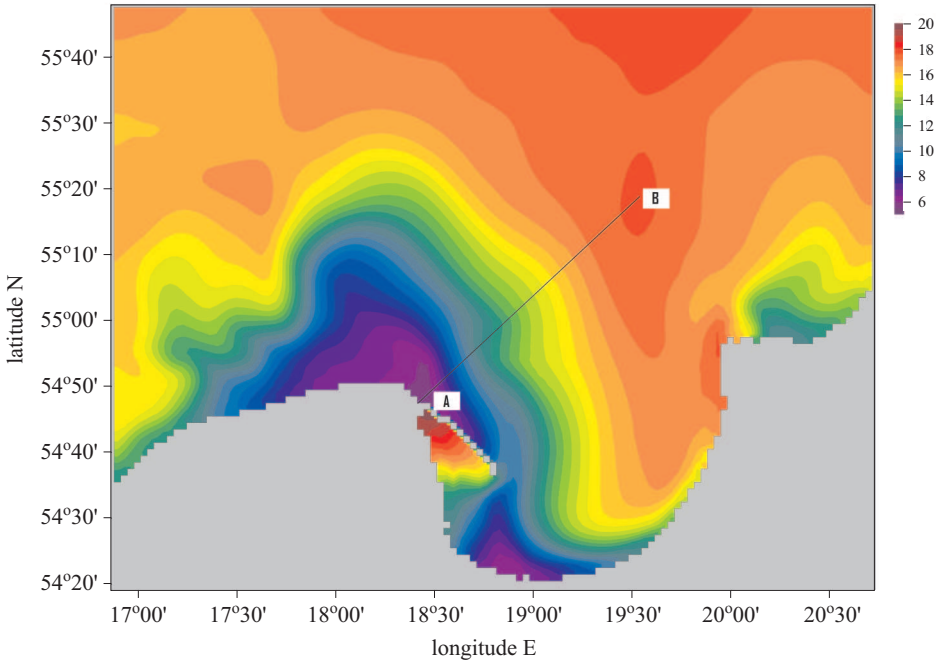

Figure 6. Calculated sea surface temperature map on 13 August 1996 showing the position of cross-section A–B

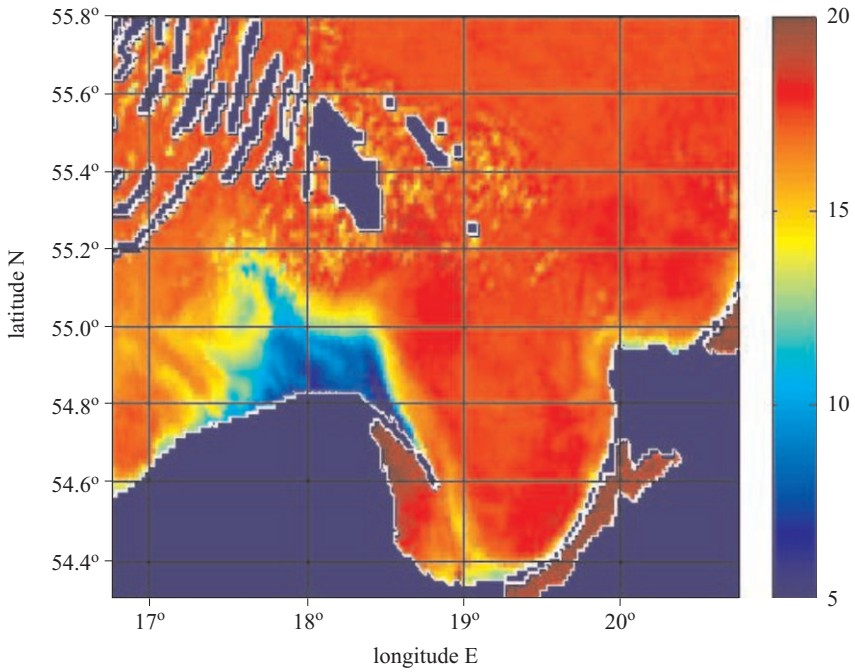

Figure 7. Satellite image of the sea surface temperature off the Hel Peninsula on 13 August 1996

The observations made on board r/v 'Baltica' on 29 August (Figure 8) revealed a very pronounced upwelling with a minimum temperature of only 9.2 degrees. According to the model there were even slightly lower temperatures towards the south-east near the Hel Peninsula (see also Figure 4). The measured temperature increased north-westwards, reaching normal summer values of about 17°C in the open sea. The model reproduced very well both the location of the coldest water, i.e. the core of the upwelling area north of the Hel Peninsula, and the gradual north-westward increase in SST.

No observations of the current dynamics in the Hel Peninsula area during August 1996 were available. So, to analyse and confirm that the gross features of our model results were correct in relation to the simulated upwelling dynamics, we checked to see how our results tallied with the classical theory of dynamics. We compared our results with estimates given by a simple, two-layer, reduced-gravity model. Being quite robust, this model takes into account the main mechanisms of upwelling dynamics: offshore Ekman drift in response to wind, and geostrophic adjustment during the formation of the coastal upwelling front. A qualitative analysis of this model is presented by Cushman-Roisin (1994). In the case of an

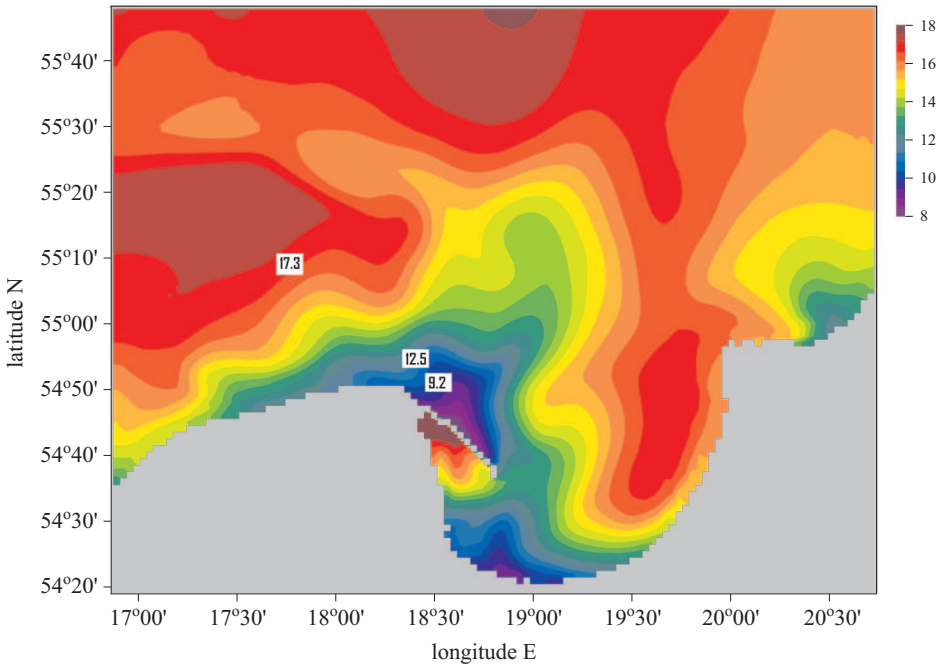

Figure 8. The calculated sea surface temperature on 29 August 1996 off the Hel Peninsula. The rectangles in the figure indicate the temperatures measured on board r/v 'Baltica'

upwelling event in its mature state, the extension of the upwelling area in the offshore direction χ_{Ek} can be estimated as:

$$\chi_{Ek} = \frac{I}{H\rho_0 f} - R, \tag{2}$$

where H is the depth of the upper layer in an undisturbed state. Here the thickness of this layer is taken to be equal to the depth of thermocline, which is of the order of the entire vertical extent of the Ekman layer, ρ_0 is the reference water density, R is the Rossby radius of deformation $R = \frac{\sqrt{g'H}}{f}$, $g' = g\frac{\Delta\rho}{\rho}$ is the reduced gravity, $\Delta\rho$ is the density difference between the two layers and f is the Coriolis parameter.

The variables on 13 August in the vicinity of the Hel Peninsula had the following orders: $H = 7$ m, $\frac{\Delta\rho}{\rho_0} = 10^{-3}$, $R \approx \frac{\sqrt{10 \times 10^{-3} \times 7}}{1 \times 10^{-4}} \approx 3$ km, $I = 28\,000$ kg m^{-1} s^{-1} (wind impulse applied to reach the full upwelling); formula (2) gives the front offshore displacement $\chi_{Ek} \approx \frac{28\,000}{7 \times 10^3 \times 10^{-4}} - 3000 = 37$ km.

Figure 9 shows the calculated distribution of the absolute vector gradient of sea surface temperature and, therefore, the location of the coastal upwelling front on 13 August. The front is located at a distance of approximately 30–40 km offshore, which is in good agreement with the estimate given by formula (2). It is important to note that the thermocline depth in the Hel Peninsula area was almost spatially uniform until the beginning of the first upwelling. This fact allows us to use formula (2).

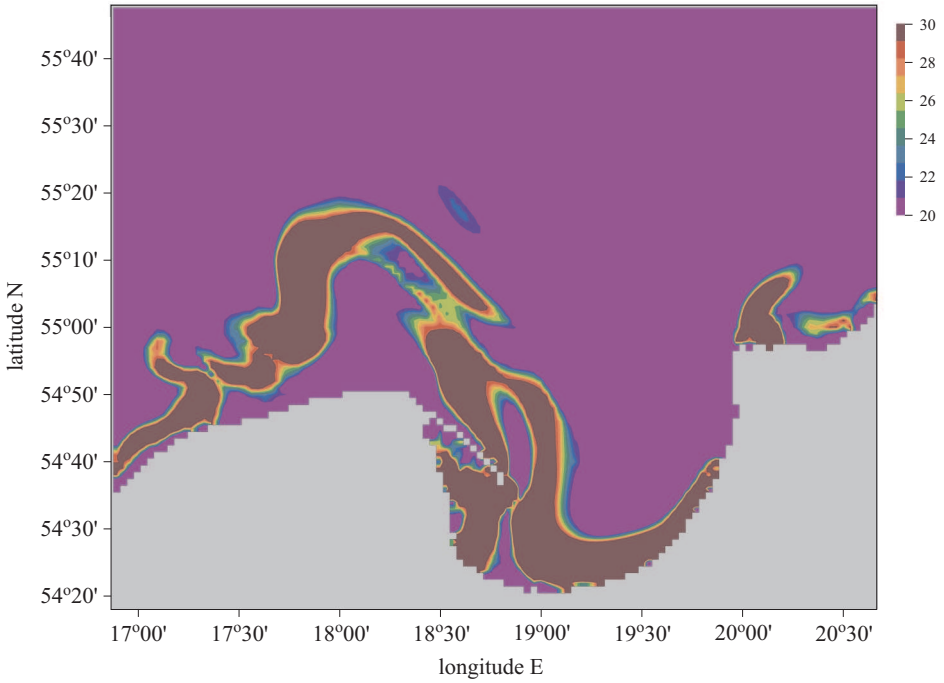

Figure 9. The absolute value of the sea surface temperature vector gradient in $^{\circ}\mathrm{C} \times 10^{-2}$ km^{-1} on 13 August 1996

On 13 August upwelling reached its culmination phase (Figure 6) and the upwelling front separated cold water (exposed and therefore stretching the lower layer) from warm water (squeezing the upper layer). Figure 10 shows the corresponding velocity field with vortices developing on both sides of the front. Figure 11 shows the corresponding sea surface elevation.

A typical feature related to coastal upwelling is the formation of an offshore-directed jet of upwelled water that extends through the SST frontal area (Cushman-Roisin 1994). The starting time of jet development is noticeable on 13 August (Figures 6 and 7) and is distinctly visible in the current and surface temperature fields on 21 August (Figures 12 and 13).

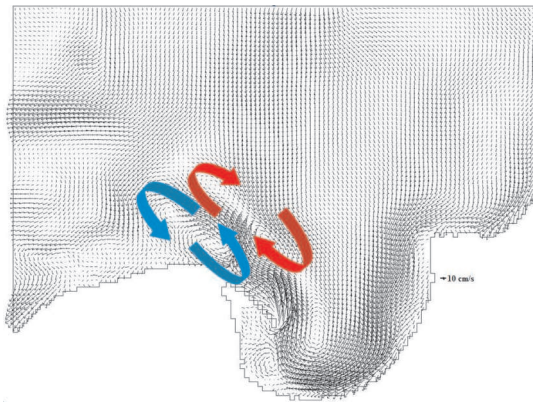

Figure 10. Velocity field at depth 10 m on 13 August 1996. The blue arrow shows the area of cyclonic vorticity, the red one the area of anticyclonic vorticity

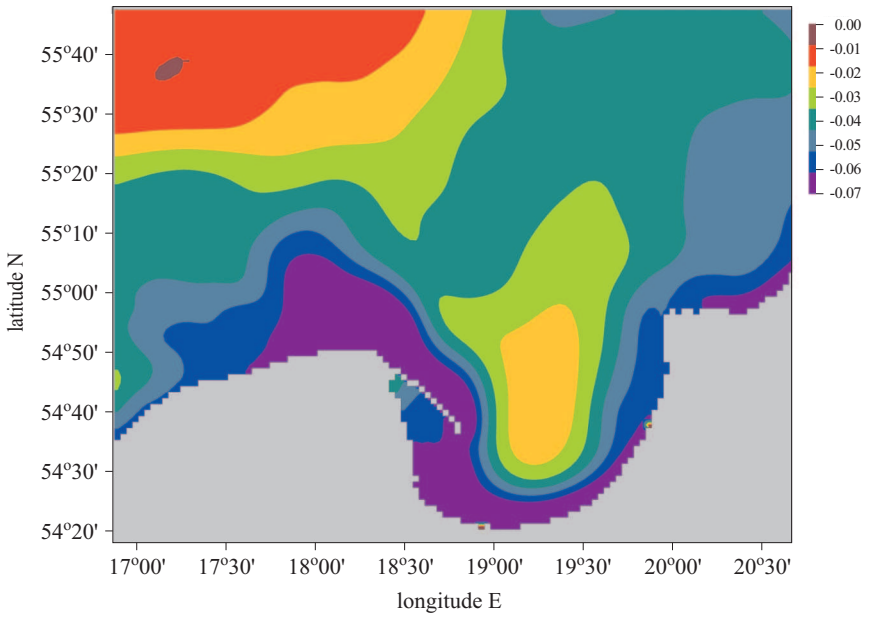

Figure 11. Sea level (in metres) on 13 August 1996

Later, on 26 August, the jet split to form pairs of counter-rotating vortices (Figure 14), while the effects of the previous upwelling on the SST smoothed towards a relatively homogeneous structure (Figure 15). A structure very similar to this jet can be found in many satellite images of the Hel Peninsula area presenting AVHRR satellite data for 2000 and 2001 (see e.g. Myrberg et al. 2008).

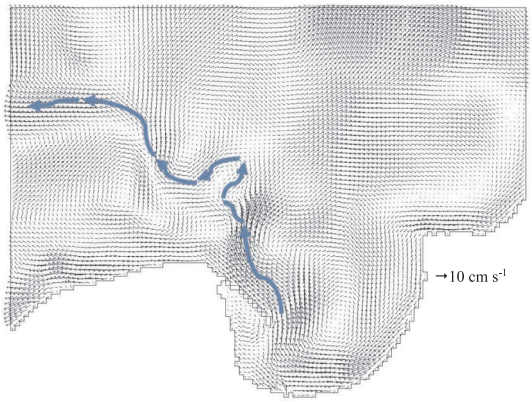

Figure 12. Surface flow field and the frontal zone (blue arrows) off the Polish coast on 21 August 1996

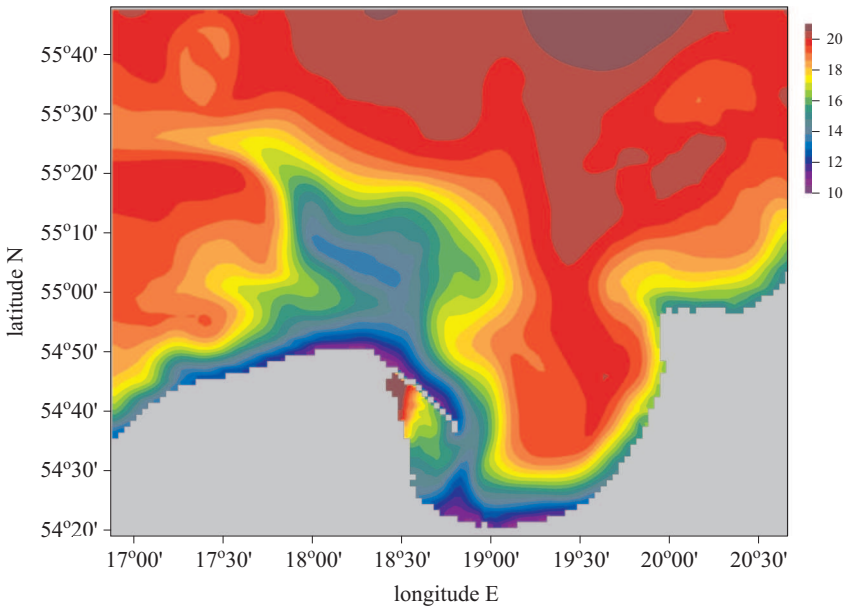

Figure 13. Sea surface temperature map on 21 August 1996

Such variability in the upwelling front is often observed in the Baltic Sea. It can be understood as an instability process of strongly sheared currents associated with upwelling. Because of the drop in sea level (Figure 11), a barotropic coastal jet develops, which is driven by coastal irregularities and the bottom topography. This jet is horizontally sheared and thus vulnerable to barotropic instability. On the other hand, the temperature gradient gives

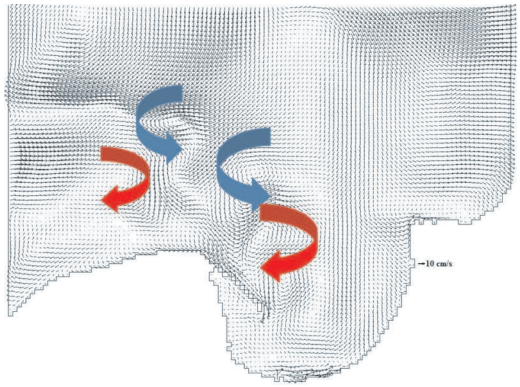

Figure 14. Surface flow field off the Polish coast on 26 August 1996. The blue arrow shows the area of cyclonic vorticity, the red one the area of anticyclonic vorticity

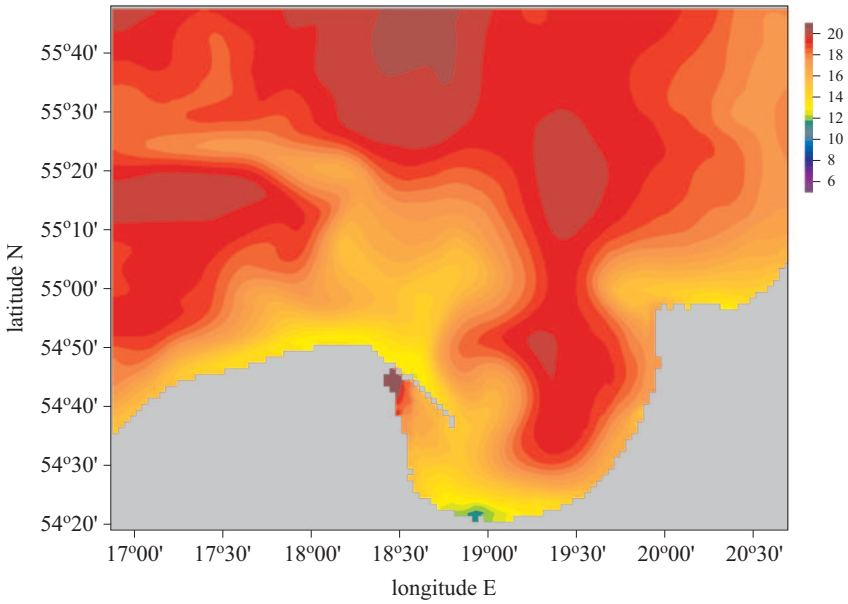

Figure 15. Sea surface temperature map on 26 August 1996

rise to a baroclinic sheared current, which is, of course, prone to baroclinic instability. According to the two-layer formulation we can say that the warm layer develops anticyclonic vorticity under the influence of vertical squeezing. On the other side of the front the exposed lower layer is vertically stretched, and cyclonic vorticity develops. This explains why mesoscale

turbulence is associated with upwelling fronts (for details, see Cushman-Roisin 1994).

3.2. The modelled upwelling events

Figure 16 shows the salinity cross-section off the Hel Peninsula. At the beginning of the analysis of the August 1996 upwelling events we will take a brief look at how upwelling is reflected in the salinity conditions near the Hel Peninsula. It becomes clear that on the open-sea side the salinity stratification is pronounced with a halocline at a depth of 55–60 m. In the upwelling area, however, the isohalines are strongly tilted; in fact, they are nearly vertical, and thus the surface salinity is about 1 per mille higher than on the open-sea side – the respective values are 8.5 and 7.5 per mille.

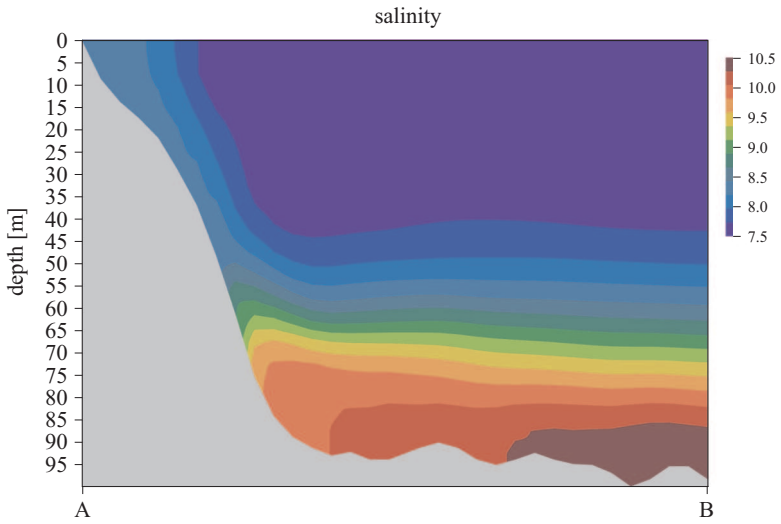

Figure 16. Salinity cross-section on 13 August 1996, as shown in Figure 6

The results of our analysis show that in August 1996 there were two conspicuous upwelling events (see Figures 3 and 4; Table 1). The favourable wind for the first upwelling blew from 7 to 16 August, the duration of this wind event being 228 hours. The SST minimum was reached on 13 August, after 160 hours of favourable wind forcing. It was precisely on 13 August that this upwelling became mature or full (Figure 6 and 17), according to Csanady's (1977) terminology. After that, the wind direction remained favourable to upwelling for another 68 hours or so but was too weak to bring about any further notable upwelling development. So, in fact the

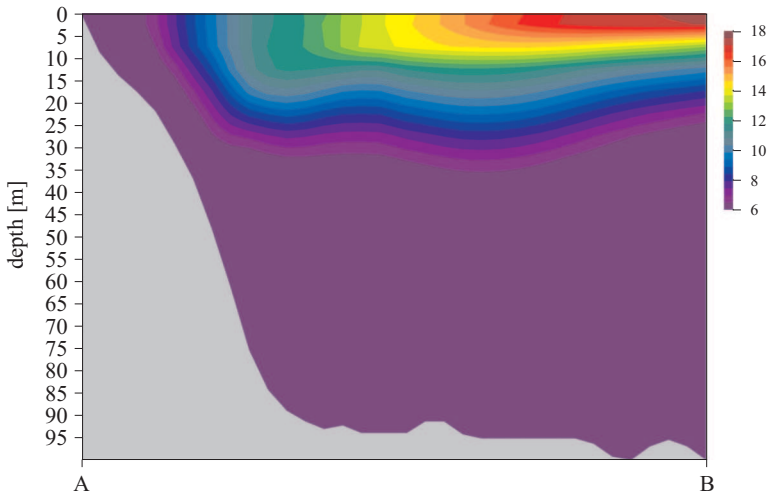

Figure 17. Temperature cross-section on 13 August 1996, as shown in Figure 6

upwelling reached its full form already after having consumed a wind impulse of 28 000 kg m^{-1} s^{-1}. During this first event, SST decreased from 18.1°C to 5.8°C (SST drop 12.3°C). The second upwelling (Figure 19) took place between 26 and 29 August. The wind impulse then was 7500 kg m^{-1} s^{-1} and the SST fell from 14.3°C to 8.8°C (SST drop 5.5°C).

This second upwelling event lasted for 42 hours. It is interesting to note that during the first upwelling it took about 85 hours for SST to fall by

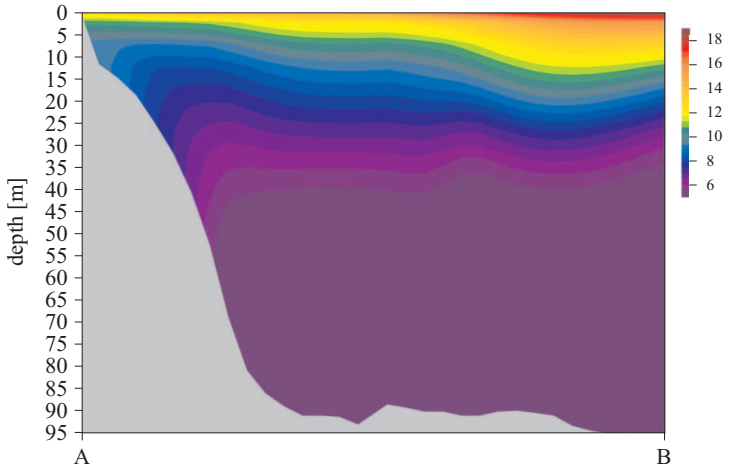

Figure 18. Temperature cross-section on 26 August 1996, as shown in Figure 6

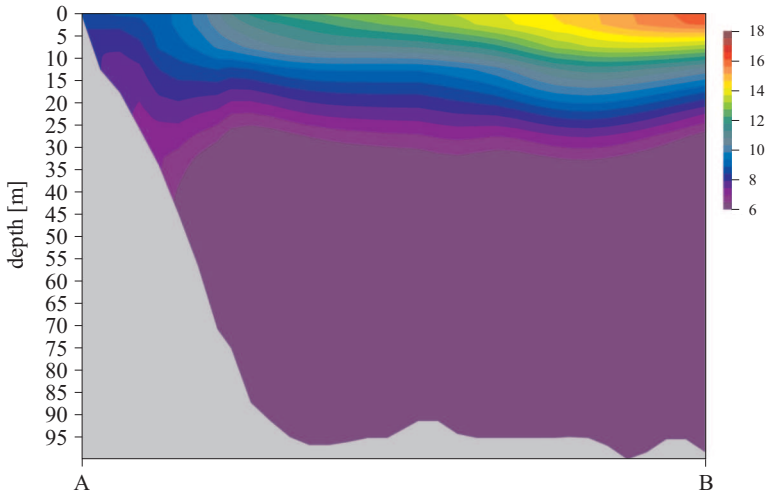

Figure 19. Temperature cross-section on 29 August 1996, as shown in Figure 6

5.5°C, which is equal to the total drop in SST during the second upwelling event. Thus, the time derivative of SST at the beginning of the first upwelling was half the value of that in the second one. The reason behind the differences in the time evolution of SST between the first and second events can be found by investigating the evolution of the vertical temperature stratification of the Hel Peninsula area. During the initial state of the first upwelling, the thermocline was at 6–10 m depth. After that, the prevailing wind became weak and/or its direction most of the time was unfavourable to upwelling development near the Hel Peninsula. Thus, the SST gradually rose from 5.5°C on 13 August to 14.3°C on 26 August. Simultaneously, the vertical structure of temperature gradually shifted back towards normal. A thin but well defined thermocline reformed in the Hel Peninsula area; it is visible in the model simulations for 26 August (Figure 18). However, the mixed layer was thinner and the stratification weaker on the Hel side in comparison to the open-sea side, where downwelling was taking place. Near the shore the thermocline depth was about 5 m. So the wind impulse required to lift this interface to the sea surface was quite small. In this case it proved to be 7500 kg m^{-1} s^{-1}. It should be borne in mind that generally in early summer, a much smaller wind impulse is needed to produce an upwelling event than in autumn, when the mixed layer can be as deep as 20 m. According to the model results, the order of the vertical velocity during both upwelling events was approximately 1.0–3.0 $\times$ 10^{-5} m s^{-1}, which can be evaluated as relatively high.

4. Summary and conclusions

This paper examines a sequence of upwelling events on the Polish coast off the Hel Peninsula in August 1996. In addition to modelling these events, the results of the simulations are compared with satellite and in situ data of sea-surface temperature; the fit is very good.

Until now, too little attention has been paid in Baltic Sea studies to the investigation of the prehistory of stratification and its role in the formation of new upwelling events. Our numerical model study has shown clearly that the intensity of such an event depends not only on the magnitude of an upwelling-favourable wind impulse but also on the temperature stratification of the water column during the initial stage of the event. When a 'chain' of upwelling events is taking place, one upwelling may play a part in forming the initial stratification for the next upwelling, as a result of which a reduced wind impulse may be enough to induce a significant drop in SST. So, in practical applications (like e.g. operational modelling) the initial stratification conditions prior to an upwelling event should be described with care in order to be able to simulate future upwelling events with good accuracy.

It has also been found that upwelling-related temperature fronts are often coupled with the development of cyclonic/anticyclonic vortices. Upwelling fronts are regions of highly sheared currents, and hence potential regions of instability. Vortices may develop from the horizontal shear of the coastal jet (barotropic instability). In addition, potential energy can also be released from the stratification when the warm layer spreads (baroclinic instability). Offshore jets of cold, upwelled waters have been observed to form near coastal irregularities; these jets cut through the front, forge their way through the warm layer, and eventually split to form pairs of counter-rotating vortices (Flament et al. 1985). Therefore, upwelling fronts are often associated with mesoscale turbulence.

Acknowledgements

We would like to thank Gisela Tschersich from BSH for making the satellite images available. We express our appreciation to Alexander Andrejev for his help in producing the figures.

References

Andrejev O., Myrberg K., Alenius P., Lundberg P. A., 2004a, *Mean circulation and water exchange in the Gulf of Finland – a study based on three-dimensional modeling*, Boreal Environ. Res., 9 (1), 1–16.

Andrejev O., Myrberg K., Lundberg P. A., 2004b, *Age and renewal time of water masses in a semi-enclosed basin – application to the Gulf of Finland*, Tellus A, 56 (5), 548–558.

Andrejev O., Myrberg K., Mälkki P., Perttilä M., 2002, *Three-dimensional modelling of the main Baltic inflow in 1993*, Environ. Chem. Phys., 24 (3), 156–161.

Andrejev O., Sokolov A., 1989, *Numerical modelling of the water dynamics and passive pollutant transport in the Neva inlet*, Meteorol. Hydrol., 12, 75–85, (in Russian).

Andrejev O., Sokolov A., 1990, *3D baroclinic hydrodynamic model and its applications to Skagerrak circulation modelling*, Proc. 17th Conf. Baltic Oceanogr., Norrköping, 38–46.

Bergström S., Carlsson B., 1994, *River runoff to the Baltic Sea: 1950–1990*, Ambio, 23 (4–5), 280–287.

Bumke K., Hasse L., 1989, *An analysis scheme for determination of true surface winds at sea from ship synoptic wind and pressure observations*, Bound.-Lay. Meteorol., 47 (1–4), 295–308.

Bunker A. F., 1976, *Computations of surface energy flux and annual air-sea interaction cycle of the North Atlantic Ocean*, Mon. Weather Rev., 104 (9), 1122–1140.

Bychkova I., Viktorov S., 1987, *Use of satellite data for identification and classification of upwelling in the Baltic Sea*, Oceanology, 27 (2), 158–162.

Csanady G. T., 1977, *Intermittent 'full' upwelling in Lake Ontario*, J. Geophys. Res., 82 (C3), 397–419.

Cushman-Roisin B., 1994, *Introduction to geophysical fluid dynamics*, Prentice-Hall, Englewood Cliffs, N. J., 320 pp.

Dietrich G. (ed.), 1972, *Upwelling in the ocean and its consequences*, Geoforum Oxford 11, Elsevier Sci./Pergamon, Frankfurt.

Fennel W., Seifert T., Kayser B., 1991, *Rossby radii and phase speeds in the Baltic Sea*, Cont. Shelf Res., 11 (1), 23–36.

Flament P., Armi L., Washburn L., 1985, *The evolving structure of an upwelling filament*, J. Geophys. Res., 90 (C6), 11 765–11 778.

Haapala J., 1994, *Upwelling and its influence on nutrient concentration in the coastal area of the Hanko Peninsula, entrance of the Gulf of Finland*, Estuar. Coast. Shelf Sci., 38 (5), 507–521.

Kochergin V. P., 1987, *Three-dimensional prognostic models*, [in:] *Three-dimensional coastal ocean models*, N. S. Heaps (ed.), Am. Geophys. Union, Coast. Estuar. Sci. Ser., 4, 201–208.

Kowalewski M., Ostrowski M., 2005, *Coastal up- and downwelling in the southern Baltic*, Oceanologia, 47 (4), 435–475.

Krężel A., Ostrowski M., Szymelfenig M., 2005, *Sea surface temperature distribution during upwelling along the Polish Baltic coast*, Oceanologia, 47 (4), 415–432.

Laanemets J., Zhurbas V., Elken J., Vahtera E., 2009, *Dependence of upwelling-mediated nutrient transport on wind forcing, bottom topography and stratification in the Gulf of Finland: model experiments*, Boreal Environ. Res., 14 (1), 213–225.

Lehmann A., Myrberg K., 2008, *Upwelling in the Baltic Sea – a review*, J. Marine Syst., 74 (Suppl. 1), S3–S12.

Leppäranta M., Myrberg K., 2009, *Physical oceanography of the Baltic Sea*, Springer Verl., Berlin–Heidelberg–New York, 378 pp.

Malicki J., Wielbińska D., 1992, *Some aspects of the atmosphere's impact on the Baltic Sea waters*, Bull. Sea Fish. Inst., 1 (125), 19–28.

Matciak M., Urbański J., Piekarek-Jankowska H., Szymelfenig M., 2001, *Presumable groundwater seepage influence on the upwelling events along the Hel Peninsula*, Oceanol. Stud., 30 (3–4), 125–132.

Mutzke A., 1998, *Open boundary condition in the GFDL-model with free surface*, Ocean Model., 116, 2–6.

Myrberg K., Andrejev O., 2003, *Main upwelling regions in the Baltic Sea: a statistical analysis based on three-dimensional modelling*, Boreal Environ. Res., 8 (2), 97–112.

Myrberg K., Andrejev O., 2006, *Modelling of the circulation, water exchange and water age properties of the Gulf of Bothnia*, Oceanologia, 48 (S), 55–74.

Myrberg K., Lehmann A., Raudsepp U., Szymelfenig M., Lips I., Lips U., Matciak M., Kowalewski M., Krężel A., Burska D., Szymanek L., Ameryk A., Bielecka L., Bradtke K., Gałkowska A., Gromisz S., Jędrasik J., Kaluźny M., Kozłowski L., Krajewska-Sołtys A., Ołdakowski B., Ostrowski M., Zalewski M., Andrejev O., Suomi I., Zhurbas V., Kauppinen O.-K., Soosaar E., Laanemets J., Uiboupin R., Talpsepp L., Golenko M., Golenko N., Vahtera E., 2008, *Upwelling events, coastal offshore exchange, links to biogeochemical processes – Highlights from the Baltic Sea Science Congress at Rostock University, Germany, 19–22 March 2007*, Oceanologia, 50 (1), 95–113.

Myrberg K., Ryabchenko V., Isaev A., Vankevich R., Andrejev O., Bendtsen J., Erichsen A., Funkquist L., Inkala A., Neelov I., Rasmus K., Rodriguez Medina M., Raudsepp U., Passenko J., Söderkvist J., Sokolov A., Kuosa H., Anderson T. R., Lehmann A., Skogen M. D., 2010, *Validation of three-dimensional hydrodynamic models of the Gulf of Finland based on a statistical analysis of a six-model ensemble*, Boreal Environ. Res., (in press).

Niiler P., Kraus E., 1977, *One-dimensional models of the upper ocean*, [in:] *Modelling and prediction of the upper layers of the ocean*, E. Kraus (ed.), Pergamon Press, Oxford, 143–172.

Orlanski I., 1976, *A simple boundary condition for unbounded hyperbolic flows*, J. Comp. Phys., 21, 251–269.

Proudman J., 1953, *Dynamical oceanography*, Methuen & Co., London, 409 pp.

Seifert T., Kayser B., 1995, *A high resolution spherical grid topography of the Baltic Sea*, Meereswiss. Ber./Mar. Sci. Rep., Inst. Ostseeforsch., Warnemünde.

Smagorinsky J., 1963, *General circulation experiments with the primitive equations. Part I: The basic experiment*, Mon. Weather Rev., 91 (3), 99–164.

Sokolov A., Andrejev O., Wulff F., Rodriguez Medina M., 1997, *The data assimilation system for data analysis in the Baltic Sea*, Syst. Ecol. Contrib., (Stockholm Univ.), 3, 66 pp.

Zhurbas V. M., Laanemets J., Vahtera E., 2008, *Modeling of the mesoscale structure of coupled upwelling/downwelling events and related input of nutrients to the upper mixed layer in the Gulf of Finland, Baltic Sea*, J. Geophys. Res., 113, C05004, doi:10.1029/2007JC004280.